

Engineering Cocrystal Solubility, Stability, and pH_{max} by Micellar Solubilization

NEAL HUANG, NAÍR RODRÍGUEZ-HORNEDO

Department of Pharmaceutical Sciences, University of Michigan, Ann Arbor, Michigan 48109-1065

Received 24 January 2011; revised 24 January 2011; accepted 13 July 2011

Published online 9 September 2011 in Wiley Online Library (wileyonlinelibrary.com). DOI 10.1002/jps.22725

ABSTRACT: Cocrystals offer great promise in enhancing drug aqueous solubilities, but face the challenge of conversion to a less soluble drug when in contact with solvent. This manuscript shows that differential solubilization of cocrystal components by micelles can impart thermodynamic stability to otherwise unstable cocrystals. The theoretical foundation for controlling cocrystal solubility and stability is presented by considering the contributions of micellar solubilization and ionization of cocrystal components. A surfactant critical stabilization concentration (CSC) and a solution pH (pH_{max}) where cocrystal and drug are thermodynamically stable are shown to characterize cocrystal stability in micellar solutions. The solubility, CSC, and pH_{max} of carbamazepine cocrystals in micellar solutions of sodium lauryl sulfate predicted by the models are in very good agreement with experimental measurements. The findings from this work demonstrate that cocrystal CSC and pH_{max} can be tailored from the selection of cofomer and solubilizing additives such as surfactants, thus providing an unprecedented level of control over cocrystal stability and solubility via solution phase chemistry. © 2011 Wiley-Liss, Inc. and the American Pharmacists Association *J Pharm Sci* 100:5219–5234, 2011

Keywords: acid–base equilibria; cocrystals; crystal engineering; solubility; stabilization; surfactants; thermodynamics; pH; micelle

INTRODUCTION

The ability to engineer the aqueous solubility of inherently insoluble pharmaceutical compounds by cocrystal formation has important implications for the development of drug delivery systems. Cocrystals owe their large solubility range to the numerous structures, diverse molecular characteristics of cocrystal components, and solution phase behavior.^{1,2} One of the fundamental consequences related to the nature of cocrystal components and their solution phase behavior is the ability to tailor the solubility–pH dependence of cocrystals of nonionizable or ionizable drugs by careful selection of cofomers and control of solution conditions. The contributions of ionization and complexation of cocrystal components to cocrystal solubility have been reported and quantitative models have been developed that allow for tailoring cocrystal solubility behavior.^{3–5} Although surfactants are

commonly used in cocrystal dissolution studies and formulations,^{6–8} and the role of micelles in drug solubilization is widely appreciated in the literature,^{9–14} their role in cocrystal solubility has been virtually unexplored.

Cocrystals that are more soluble than the parent drug can transform, sometimes very rapidly, to a less soluble drug upon contact with solution.^{15–18} Thus, understanding and controlling cocrystal thermodynamic stability is essential if they are to become pharmaceutical products.

We recently showed that surfactants can impart thermodynamic stability to cocrystals that are otherwise unstable in solution.^{19,20} A surfactant critical stabilization concentration (CSC) was discovered where cocrystal and drug phases became thermodynamically stable in micellar solutions. Below CSC, cocrystals are thermodynamically unstable, whereas at CSC and above, cocrystals are thermodynamically stable. A theoretical treatment predicted that the stabilizing effect of micellar surfactants is related to their differential solubilization of cocrystal components. In other words, when a surfactant system has superior solubilization power for the least soluble cocrystal component, its effectiveness as a cocrystal

Additional Supporting Information may be found in the online version of this article. Supporting Information

Correspondence to: Nair Rodríguez-Hornedo (Telephone: +734-763-0101; Fax: +734-615-6162; E-mail: nrh@umich.edu)

Journal of Pharmaceutical Sciences, Vol. 100, 5219–5234 (2011)

© 2011 Wiley-Liss, Inc. and the American Pharmacists Association

stabilizer increases. These findings extend to multiple additives and solubilization mechanisms, including complexing agents and polymers.

The work presented here establishes the contributions of micellar solubilization and ionization of cocrystal components on cocrystal solubility, develops mathematical models that predict cocrystal solubility behavior in terms of thermodynamic parameters that are readily available in the literature or experimentally accessible, and provides a mechanistic basis for tailoring cocrystal CSC and pH_{max} to meet solubility and stability requirements.

This work shows for the first time that micellar solubilization can induce a pH_{max} for cocrystals that do not have one otherwise. Mathematical models are derived that describe the dependence of cocrystal solubility, CSC, and pH_{max} on cocrystal solubility product (K_{sp}), components $K_{\text{s}}(\text{s})$ and $K_{\text{a}}(\text{s})$, and micellar surfactant concentration.

The predictive power of the models is evaluated from studies that examine the influence of a surfactant (sodium lauryl sulfate, SLS) and coformer ionization on cocrystal solubility, stability, and CSC for a range of cocrystals of a hydrophobic, nonionizable drug (carbamazepine, CBZ) and hydrophilic coformers with several ionization properties and stoichiometries. The cocrystals studied include the following: 1:1 carbamazepine–salicylic acid (CBZ–SLC), 1:1 carbamazepine–saccharin (CBZ–SAC), 2:1 carbamazepine–succinic acid (CBZ–SUC), and 2:1 carbamazepine–4-aminobenzoic acid monohydrate (CBZ–4ABA–HYD). The selected cocrystals cover the two most abundant stoichiometries, and the coformers have ionization properties common among reported cocrystals. SLC and SAC are monoprotic weak acids; SLC has a reported pK_{a} of 3.0,²¹ SAC has a range of reported pK_{a} values between 1.8 and 2.2.^{22,23} SUC is a diprotic weak acid with pK_{a} values of 4.1 and 5.6.²⁴ 4ABA is amphoteric with pK_{a} values of 2.6 and 4.8.²⁵

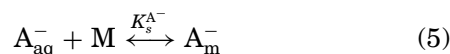
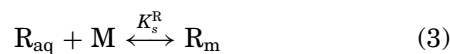
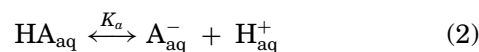
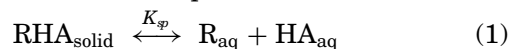
THEORETICAL

This section describes the theoretical basis of our quantitative approach to predict cocrystal solubilization and thermodynamic stability from solution phase properties of cocrystal components and micellar surfactants. We first present the solution phase equilibria that govern the solubilization properties of cocrystals in micellar solutions. Relatively simple equations to calculate cocrystal solubility are derived by considering the contributions of ionization and micellar solubilization of cocrystal components. Several important physicochemical factors are identified that can be used to make cocrystal solubility and stability predictions.

The interested reader is directed to the supporting information for derivations of the equations presented in this section. The analysis can be generalized to mixed micelles and other solubilization mechanisms, although they may be of a different nature.

Cocrystal Solubilization and Thermodynamic Stabilization in Micellar Solutions

A micellar solution phase in equilibrium with a solid cocrystal phase consists of molecules of cocrystal components and surfactant in several states of self-association, complexation, and ionization. Surfactants self-assemble in solution at a critical micellar concentration (CMC) and provide a means to solubilize cocrystal components. The solubility of a cocrystal (RHA) composed of the nonionized forms of its components, a nonionizable drug (R) and an ionizable coformer, in this case, a monoprotic weak acid (HA), is described by the equilibria for cocrystal dissociation, ionization, complexation, and micellar solubilization. For the sake of simplicity, solution complexation of cocrystal components is assumed to be negligible and the expressions for other equilibria are



where subscripts m and aq refer to micellar and aqueous pseudophases, respectively. K_{sp} is the cocrystal solubility product and K_{a} is the dissociation constant for acidic coformer. M is the micellar surfactant. K_{s}^{R} , K_{s}^{HA} , and $K_{\text{s}}^{\text{A}^{-}}$ are the micellar solubilization constants for cocrystal components and their ionized forms.

The cocrystal solubility, $S_{\text{RHA,T}}$, under stoichiometric conditions, is equal to the total concentration of each cocrystal component in equilibrium with the solution, $S_{\text{RHA,T}} = [\text{R}]_{\text{T}} = [\text{A}]_{\text{T}}$. The contributions of ionization and micellar solubilization of each cocrystal component to the solubility of a cocrystal RHA is given by

$$\begin{aligned} S_{\text{RHA,T}} &= [\text{R}]_{\text{aq}} + [\text{R}]_{\text{m}} \\ &= [\text{HA}]_{\text{aq}} + [\text{A}^{-}]_{\text{aq}} + [\text{HA}]_{\text{m}} + [\text{A}^{-}]_{\text{m}} \quad (6) \end{aligned}$$

An expression for cocrystal solubility in terms of experimentally accessible solution properties is

obtained:

$$S_{\text{RHA},T} = \sqrt{K_{\text{sp}} (1 + K_{\text{s}}^{\text{R}} [\text{M}]) \left(1 + \frac{K_{\text{a}}}{[\text{H}^+]} + K_{\text{s}}^{\text{HA}} [\text{M}] + \frac{K_{\text{a}}}{[\text{H}^+]} K_{\text{s}}^{\text{A}^-} [\text{M}] \right)} \quad (7)$$

by combining Equation 6 with the equilibrium constant equations below:

$$K_{\text{sp}} = [\text{R}]_{\text{aq}} [\text{HA}]_{\text{aq}} \quad (8)$$

$$K_{\text{a}} = \frac{[\text{A}^-]_{\text{aq}} [\text{H}^+]_{\text{aq}}}{[\text{HA}]_{\text{aq}}} \quad (9)$$

$$K_{\text{s}}^{\text{R}} = \frac{[\text{R}]_{\text{m}}}{[\text{R}]_{\text{aq}} [\text{M}]} \quad (10)$$

$$K_{\text{s}}^{\text{HA}} = \frac{[\text{HA}]_{\text{m}}}{[\text{HA}]_{\text{aq}} [\text{M}]} \quad (11)$$

$$K_{\text{s}}^{\text{A}^-} = \frac{[\text{A}^-]_{\text{m}}}{[\text{A}^-]_{\text{aq}} [\text{M}]} \quad (12)$$

where the terms in brackets refer to concentrations, with the recognition that under dilute solution conditions they approximate activities.

Equation 7 can be further simplified to

$$S_{\text{RHA},T} = \sqrt{K_{\text{sp}} (1 + K_{\text{s}}^{\text{R}} [\text{M}]) \left(1 + \frac{K_{\text{a}}}{[\text{H}^+]} + K_{\text{s}}^{\text{HA}} [\text{M}] \right)} \quad (13)$$

when $K_{\text{s}}^{\text{HA}} \gg K_{\text{s}}^{\text{A}^-}$, and the micellar solubilization of ionized species negligibly affects total solubility unless present at very high concentrations.^{26–28} Equation 13 predicts that cocrystal solubility increases with increasing cocrystal K_{sp} , components K_{s}^{R} and K_{s}^{HA} , cofomer ionization $K_{\text{a}}/[\text{H}^+]$, and surfactant micellar concentration, $[\text{M}]$.

It is evident from Equations 7 and 13 that cocrystal solubility is not linearly dependent on micellar concentration. This is in contrast to the well-known linear dependence of the micellar solubilization of a single-component solid phase of a nonionizable drug R:

$$S_{\text{R},T} = S_{\text{R},\text{aq}} (1 + K_{\text{s}}^{\text{R}} [\text{M}]) \quad (14)$$

where $S_{\text{R},\text{aq}}$ is the solubility of crystal R in the aqueous pseudophase. In this analysis, K_{s} values are assumed to be independent of solute and surfactant concentrations.

Equations 13 and 14 are shown graphically in Figure 1 for the case of a nonionizable, hydrophobic drug and its cocrystal with an ionizable, hydrophilic cofomer where $K_{\text{s}}^{\text{HA}} = 0$. This plot reveals that cocrystal and drug solubility surfaces intersect along a curve

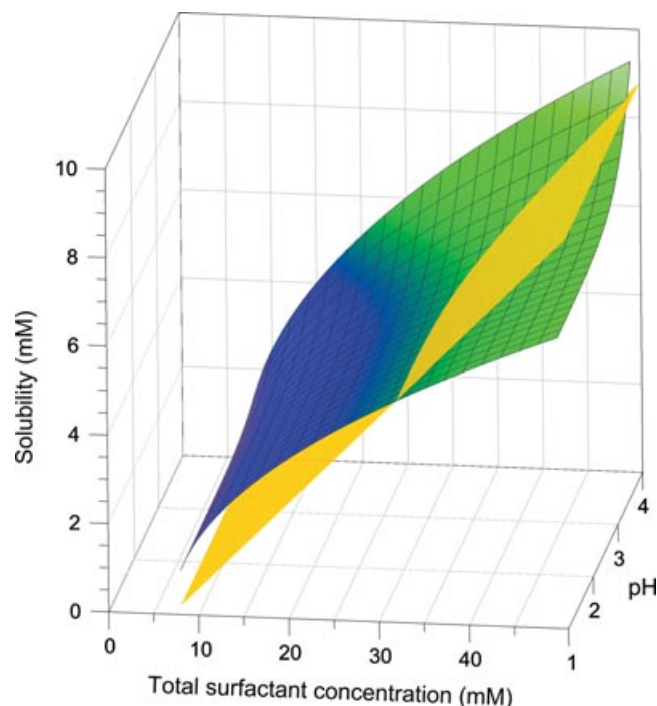


Figure 1. Cocrystal RHA (blue/green surface) and drug R (yellow surface) solubility dependence on surfactant concentration and pH. The intersection of the cocrystal and drug solubility surfaces represents the surfactant concentrations (CSC) and pH values (pH_{max}), where cocrystal and drug are in thermodynamic equilibrium with the solution. Solubilities were calculated from Equations 13 and 14, with $K_{\text{sp}} = 1 \text{ mM}^2$ ($S_{\text{RHA},\text{aq}}/S_{\text{R},\text{aq}} = 5$), $S_{\text{R},\text{aq}} = 0.2 \text{ mM}$, $\text{p}K_{\text{a}} = 4$, $K_{\text{s}}^{\text{R}} = 1 \text{ mM}^{-1}$, $K_{\text{s}}^{\text{HA}} = 0$, and $\text{CMC} = 8 \text{ mM}$.

of given surfactant concentration and pH values and identifies stability regions for cocrystal or drug by two critical parameters. The first is the CSC or the surfactant concentration where cocrystal and drug solid phases are in equilibrium with the solution. The second is the pH_{max} or the pH value at the CSC. Below the CSC or above pH_{max} , the cocrystal is thermodynamically unstable and conversion to solid drug is favorable. Above the CSC or below pH_{max} , the cocrystal becomes the thermodynamically stable phase, and conversion to solid drug is not possible. Cocrystal formation in this region is, however, favorable in the presence of a cofomer. When one or more cocrystal components ionize, both CSC and pH_{max} are necessary to describe the solution conditions under which cocrystal and/or drug solid phase are thermodynamically stable.

The existence of CSC and pH_{max} (in the case of ionizable cocrystal component) is a consequence of the lower rate of increase of cocrystal solubility with surfactant concentration as compared with that of drug solubility. It is evident from Equations 13 and 14 that cocrystal solubility depends on $\sqrt{[\text{M}]}$ (when $K_{\text{s}}^{\text{HA}} = 0$), whereas the drug solubility depends on $[\text{M}]$.

Estimation of Cocrystal Solubilization from Drug Solubilization

A useful estimate of the surfactant influence on cocrystal solubilization can be calculated from the knowledge of the drug solubilization according to

$$\frac{S_{\text{RHA},\text{T}}}{S_{\text{RHA},\text{aq}}} = \sqrt{\frac{S_{\text{R},\text{T}}}{S_{\text{R},\text{aq}}}} \quad (15)$$

This expression is obtained by combining Equations 13 and 14 for a nonionizable drug R when K_s^{R} is unaffected by the coformer and $K_s^{\text{HA}} = 0$. A surfactant concentration that increases drug solubility by 100-fold is predicted to increase cocrystal solubility by 10-fold. Equation 15 implies that a surfactant will increase the solubility of all 1:1 cocrystals of a drug by the same ratio as long as the stated assumptions are justified.

Equation 15 can be rewritten for a general cocrystal stoichiometry, R_nX_m , as

$$\frac{S_{R_nX_m,\text{T}}}{S_{R_nX_m,\text{aq}}} = \left(\frac{S_{\text{R},\text{T}}}{S_{\text{R},\text{aq}}} \right)^{\frac{n}{n+m}} \quad (16)$$

for a nonionizable drug R and coformer X. The solubility increase for a 2:1 cocrystal is predicted to be $100^{2/3}$ or 21.5-fold its aqueous solubility when the drug solubility is increased by 100-fold. Thus cocrystal stoichiometries richer in hydrophobic drug will exhibit a weaker dependence of total cocrystal solubility on micellar solubilization, leading to higher CSC or pH_{max} values.

Mechanism by Which Micelles Stabilize Cocrystals

The influence of micellar solubilization on cocrystal thermodynamic stability and CSC can be explained by considering the species distribution in micellar solutions at equilibrium with cocrystal and/or drug solid phases. Figure 2 shows the distribution of the drug in micellar and aqueous environments for a crystal of a hydrophobic drug R and its cocrystal with a hydrophilic coformer HA under nonionizing conditions where $K_s^{\text{HA}} = 0$.

When drug crystal phase (R) is in equilibrium with the micellar solution, the drug concentration in the aqueous environment, $[R]_{\text{R},\text{aq}}$, remains constant with increasing surfactant concentration. At surfactant concentrations above CMC, the drug concentration in the micellar environment, $[R]_{\text{R},\text{m}}$, increases linearly. For cocrystal (RHA) in equilibrium with the micellar solution (where drug is solubilized by the micelle and the coformer is not), the drug concentration in the aqueous environment, $[R]_{\text{RHA},\text{aq}}$, is not constant, but decreases with increasing surfactant concentration above CMC. Because the coformer is not solubilized by the micelle, the aqueous phase becomes enriched with

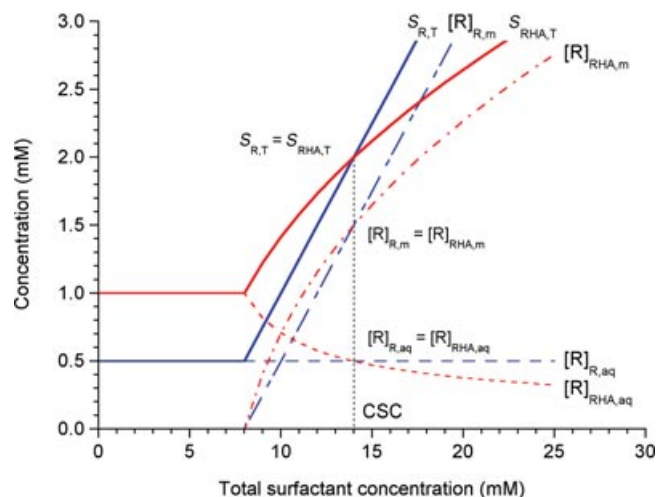


Figure 2. Distribution of drug (R) between the aqueous and micellar environments in surfactant solutions at equilibrium with the cocrystal (RHA) and crystal (R). The cocrystal thermodynamic stability relative to the drug decreases with surfactant concentration. A thermodynamically unstable cocrystal in pure solvent becomes stable at the CSC where all curves intersect. Cocrystal is more soluble than the drug below CSC, equally soluble to drug at CSC, and less soluble than the drug above CSC. Subscripts aq, m, and T, refer to aqueous, micellar, and total. Solubilities and drug distributions were calculated from Equations 13 and 14, with $K_{\text{sp}} = 1 \text{ mM}^2$, $K_s^{\text{R}} = 0.5 \text{ mM}^{-1}$, $K_s^{\text{HA}} = 0$, $S_{\text{R},\text{aq}} = 0.5 \text{ mM}$, and $\text{CMC} = 8 \text{ mM}$.

coformer and $[R]_{\text{RHA},\text{aq}}$ decreases to maintain a constant solubility product as described by the cocrystal dissociation equilibrium. This imbalance of cocrystal components in the aqueous environment dampens the increase in the total cocrystal solubility, as drug solubilized by the micelle increases with surfactant concentration. A CSC where cocrystal is in equilibrium with the drug is reached as indicated by the intersection of the total drug concentration curves, $[R]_{\text{RHA},\text{T}} = [R]_{\text{R},\text{T}}$, as well as the speciation in the aqueous and micellar environments, $[R]_{\text{RHA},\text{aq}} = [R]_{\text{R},\text{aq}}$ and $[R]_{\text{RHA},\text{m}} = [R]_{\text{R},\text{m}}$.

CSC and pH_{max} Dependence on Cocrystal and Surfactant Properties

Cocrystals with higher solubilities in water are predicted to exhibit higher CSC values as illustrated in Figure 3. For cocrystals of the same drug, aqueous solubilities can be altered by different coformers or by coformer ionization behavior in solution (by adjusting solution pH).

The influence of cocrystal aqueous solubility on CSC may be calculated from

$$\text{CSC} = \frac{\left(\frac{S_{\text{RHA},\text{aq}}}{S_{\text{R},\text{aq}}} \right)^2 - 1}{K_s^{\text{R}}} + \text{CMC} \quad (17)$$

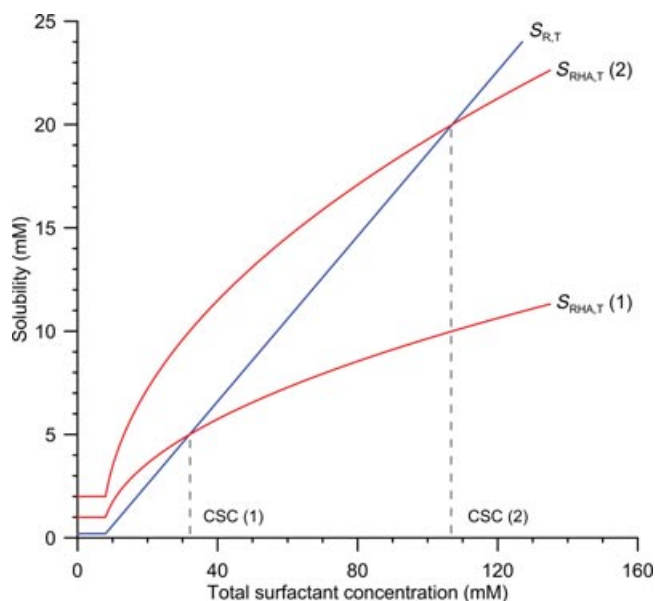


Figure 3. Influence of surfactant solubilization on cocystal solubility and CSC for cocystals of the same drug with different aqueous solubilities. More soluble cocystals relative to the drug require higher surfactant concentrations to achieve CSC. Total solubilities of cocystal RHA ($S_{RHA,T}$) and drug ($S_{R,T}$) were calculated from Equations 13 and 14, with cocystal $K_{sp} = 1$ and 4 mM^2 ($S_{RHA,aq}/S_{R,aq} = 5$ and 10), $S_{R,aq} = 0.2 \text{ mM}$, $K_s^R = 1 \text{ mM}^{-1}$, $K_s^{HA} = 0$, and $\text{CMC} = 8 \text{ mM}$.

by solving for the surfactant concentration at which $S_{RHA,T} = S_{R,T}$, from Equations 13 and 14. This expression applies to a 1:1 cocystal with no micellar solubilization of cofomer and negligible solution complexation of cocystal components.

The influence of the drug and cofomer micellar solubilization on CSC had been recently presented.^{19,20} The basis for the existence of the CSC for cocystal and drug was described from the differential micellar solubilization of the drug and the cofomer. The greater the drug micellar solubilization, K_s^R , relative to that of the cofomer, K_s^{HA} , the lower is the CSC value. In the case of pharmaceutical cocystals, drugs are generally much more hydrophobic than cofomers and $K_s^R \gg K_s^{HA}$.

Figure 4 shows the dependence of CSC on drug micellar solubilization (K_s^R) and cocystal aqueous solubility, as predicted by Equation 17. CSC is inversely proportional to drug micellar solubilization and directly proportional to cocystal aqueous solubility. This equation allows for estimation of the required K_s^R to achieve the CSC for the cocystal and its drug component, and in this way, provide guidance for the rational selection of surfactant and concentration. The choice of the right surfactant or combination of surfactants and additives will depend on the desired solubility advantage of cocystal over drug and the time over which it is to be sustained. In some cases,

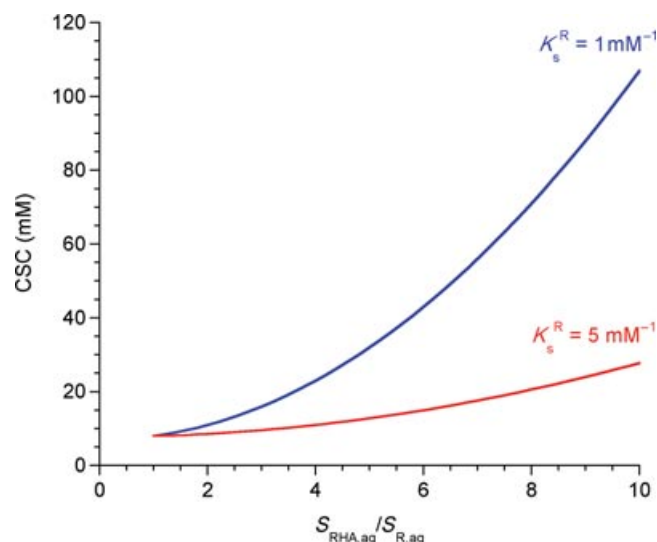


Figure 4. The CSC increases with increasing cocystal to drug solubility ratio in pure water (or below CMC) and with decreasing drug micellar solubilization, K_s^R . CSC calculated from Equation 17, with $K_s^{HA} = 0$ and $\text{CMC} = 8 \text{ mM}$.

lowering the solubility advantage by a small fraction may protect cocystals from conversion, whereas in others, a longer stability may be desired and conditions closer to the CSC required. Cocystals can impart a response to environmental conditions that the drug lacks, for example, pH sensitivity, and in this way, provide opportunities for enhanced drug delivery besides solubility alone.

Micellar solubilization of cocystal components can also impart pH_{max} to a cocystal that otherwise does not have one, as shown in Figure 5. The solubility–pH dependence for a cocystal RHA of a nonionizable drug and a weakly acidic cofomer, where the cocystal is more soluble than drug R at all pH values, is presented in Figure 5a. Many CBZ cocystals, including CBZ–SAC, CBZ–SLC, and CBZ–4ABA–HYD, have been shown to exhibit this behavior and, consequently, have no pH_{max} in water.^{4,29,30} This behavior, however, is changed by micellar solubilization and ionization of cocystal components (Fig. 5b), where the cocystal and drug solubility curves intersect at a given pH, or pH_{max} . The surfactant concentration at this intersection is the CSC. The drug micellar solubilization leading to cofomer enrichment in the aqueous environment is responsible for the CSC and pH_{max} .

Considering the contributions of cofomer solubilization and ionization in addition to drug solubilization, leads to a more general form of Equation 17 expressed by

$$\text{CSC} = \frac{\frac{K_{sp}}{S_{R,aq}^2} \left(1 + \frac{K_a}{[\text{H}^+]} \right) - 1}{K_s^R - \frac{K_{sp}}{S_{R,aq}^2} K_s^{HA}} + \text{CMC} \quad (18)$$

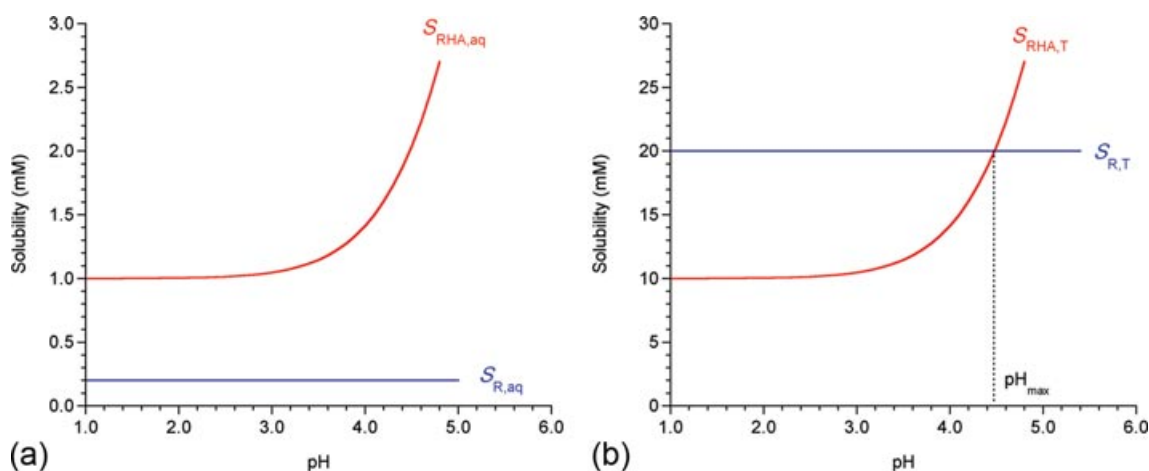


Figure 5. pH_{max} of a cocrystal can be tailored by micellar solubilization of cocrystal components. Solubility–pH dependence for a cocrystal RHA and drug R (a) in water and (b) in a micellar solution. Calculations are based on Equation 18, with $K_{\text{sp}} = 1 \text{ mM}^2$ ($S_{\text{RHA,aq}}/S_{\text{R,aq}} = 5$), $S_{\text{R,aq}} = 0.2 \text{ mM}$, $[\text{M}] = 99 \text{ mM}$ ($S_{\text{R,T}}/S_{\text{R,aq}} = 100$ and $S_{\text{RHA,T}}/S_{\text{RHA,aq}} = 10$), $\text{p}K_{\text{a}} = 4$, $K_{\text{s}}^{\text{R}} = 1 \text{ mM}^{-1}$, and $K_{\text{s}}^{\text{HA}} = 0$.

where $[\text{H}^+]$ represents $[\text{H}^+]_{\text{max}}$. According to Equation 18, the CSC for a 1:1 cocrystal RHA is dependent on several critical parameters: $K_{\text{sp}}/S_{\text{R,aq}}^2$, K_{a} , $[\text{H}^+]$, K_{s}^{R} , and K_{s}^{HA} . This equation can also be solved for $[\text{H}^+]$ to predict the pH_{max} dependence on micellar surfactant concentration and other cocrystal and surfactant properties. Equation 18 and Figure 6 show that if a CSC exists, there is also a pH_{max} value associated with that CSC and vice versa. CSC is predicted to increase as ionization increases. Higher levels of ionization increase cocrystal solubility and, thus, more surfactant is required to achieve the CSC. Equation 18 can also be used to engineer a cocrystal pH_{max} based on selection of an appropriate surfactant and concentration.

Table 1 summarizes the equations that describe cocrystal solubility and CSC for several common classes of cocrystals with varying stoichiometries and component ionization properties.

The theoretical treatment of cocrystal micellar solubilization suggests that the CSC where cocrystal and drug phases are in thermodynamic equilibrium is most readily achieved by (1) preferential drug solubilization ($K_{\text{s}}^{\text{R}} \gg K_{\text{s}}^{\text{HA}}$), (2) cocrystals of lower aqueous solubility relative to drug, and (3) cocrystal stoichiometries that are higher in coformer.

MATERIALS AND METHODS

Materials

Anhydrous monoclinic CBZ(III) (lot #057K11612 US-Pharmacopeia grade) was purchased from Sigma Chemical Company (St. Louis, Missouri), stored at 5°C over anhydrous calcium sulfate, and used as received. SLC (lot #09004LH), SAC (lot #03111DD),

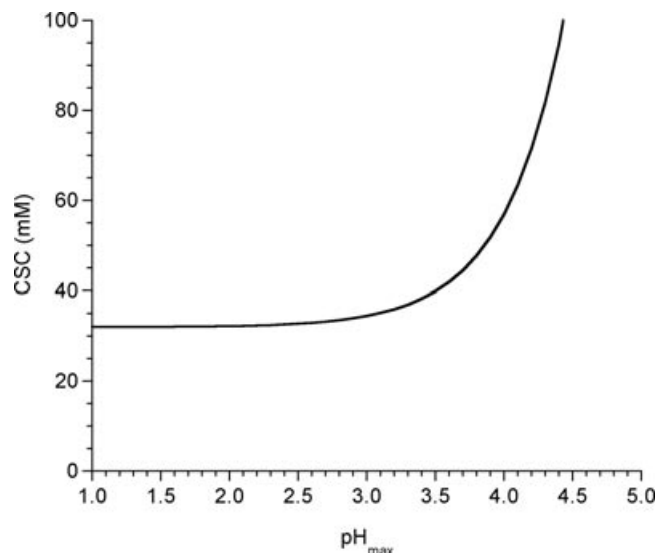


Figure 6. Critical stabilization concentration dependence on pH_{max} according to Equation 18 for a cocrystal RHA. CSC increases greatly at pH above the coformer $\text{p}K_{\text{a}}$ (i.e., increased ionization). Calculations are based on Equation 18, with $K_{\text{sp}} = 1 \text{ mM}^2$, $S_{\text{R,aq}} = 0.2 \text{ mM}$, $K_{\text{s}}^{\text{R}} = 1 \text{ mM}^{-1}$, $K_{\text{s}}^{\text{HA}} = 0$, $\text{p}K_{\text{a}} = 4$, and $\text{CMC} = 8 \text{ mM}$.

SUC (lot #037K0021), 4ABA (lot #068K0698), and SLS (lot #104H0667) were also purchased from Sigma Chemical Company and used as received. Water used in this study was filtered through a double deionized purification system (Milli Q Plus Water System from Millipore Company, Bedford, Massachusetts).

Cocrystal Synthesis

Cocrystals were prepared by reaction crystallization method at room temperature by adding CBZ to nearly saturated solutions of coformer.¹⁶ CBZ–SLC was

Table 1. Equations that Describe Cocrystral Solubility and CSC as a Function of Cocrystral K_{sp} , Components K_a and K_s , Solution $[H^+]$, Surfactant Micellar Concentration $[M]$ and CMC

Cocrystral	Solubility	Equation	CSC	Equation
RHA 1:1 nonionizable: monoprotic acid	$S_{RHA,T} = \sqrt{K_{sp} \left(1 + K_S^R [M] \right) \left(1 + \frac{K_a}{[H^+]} + K_S^{HA} [M] \right)}$	(13)	$CSC = \frac{\frac{K_{sp}}{S_{R, aq}^3} \left(1 + \frac{K_a}{[H^+]} \right) - 1}{K_S^R - \frac{K_{sp}}{S_{R, aq}^3} K_S^{HA}} + CMC$	(18)
HXHA 1:1 monoprotic acid: monoprotic acid	$S_{HXHA,T} = \sqrt{K_{sp} \left(1 + \frac{K_{HX}^{HX}}{[H^+]} + K_S^{HX} [M] \right) \left(1 + \frac{K_a^{HA}}{[H^+]} + K_S^{HA} [M] \right)}$	(19)	$CSC = \frac{\frac{K_{sp}}{S_{HX, aq}^3} \left(1 + \frac{K_a^{HA}}{[H^+]} \right) - \left(1 + \frac{K_{HX}^{HX}}{[H^+]} \right)}{K_S^{HX} - \frac{K_{sp}}{S_{HX, aq}^3} K_S^{HA}} + CMC$	(20)
BHA 1:1 monoprotic basic: monoprotic acid	$S_{BHA,T} = \sqrt{K_{sp} \left(1 + \frac{[H^+]}{K_S^B} + K_S^B [M] \right) \left(1 + \frac{K_a^{HA}}{[H^+]} + K_S^{HA} [M] \right)}$	(21)	$CSC = \frac{\frac{K_{sp}}{S_{B, aq}^3} \left(1 + \frac{K_a^{HA}}{[H^+]} \right) - \left(1 + \frac{[H^+]}{K_S^B} \right)}{K_S^B - \frac{K_{sp}}{S_{B, aq}^3} K_S^{HA}} + CMC$	(22)
R ₂ H ₂ A 2:1 nonionizable: diprotic acid	$S_{R_2H_2A,T} = \sqrt[3]{\frac{K_{sp}}{4} \left(1 + K_S^R [M] \right)^2 \left(1 + \frac{K_a^{H_2A}}{[H^+]} + \frac{K_a^{H_2A} K_a^{HA^-}}{[H^+]^2} + K_S^{H_2A} [M] \right)}$	(23)	$CSC = \frac{\frac{2K_{sp}}{S_{R_2, aq}^3} \left(1 + \frac{K_a^{H_2A}}{[H^+]} + \frac{K_a^{H_2A} K_a^{HA^-}}{[H^+]^2} \right) - 1}{K_S^R - \frac{2K_{sp}}{S_{R_2, aq}^3} K_S^{H_2A}} + CMC$	(24)
R ₂ HAB 2:1 nonionizable: amphoteric	$S_{R_2HAB,T} = \sqrt[3]{\frac{K_{sp}}{4} \left(1 + K_S^R [M] \right)^2 \left(1 + \frac{[H^+]}{K_a^{H_2AB^+}} + \frac{K_a^{HAB}}{[H^+]} + K_S^{HAB} [M] \right)}$	(25)	$CSC = \frac{\frac{2K_{sp}}{S_{R_2, aq}^3} \left(1 + \frac{[H^+]}{K_a^{H_2AB^+}} + \frac{K_a^{HAB}}{[H^+]} \right) - 1}{K_S^R - \frac{2K_{sp}}{S_{R_2, aq}^3} K_S^{HAB}} + CMC$	(26)

prepared in acetonitrile, CBZ–SAC and CBZ–SUC were prepared in ethanol, and CBZ–4ABA–HYD was prepared in water. CBZ dihydrate (CBZD) was prepared in water. Solid phases were characterized by X-ray powder diffraction (XRPD).

CSC Measurement from Solid Phase Stability (Method 1)

Cocrystals were suspended in aqueous solutions of different SLS concentrations. Suspensions were seeded with approximately 5% (w/w) of CBZD after several hours. CBZ–SLC or CBZ–SAC (30–40 mg) was added to 3 mL of aqueous SLS solution. CBZ–SUC or CBZ–4ABA–HYD (70–80 mg) was added to 3 mL of aqueous SLS solution. Samples were maintained at $25 \pm 0.1^\circ\text{C}$ for a duration of 3 days, when the solids were recovered and analyzed by XRPD. Examination of the XRPD patterns revealed that 24 h was sufficient for the samples to reach equilibrium. The CSC was determined to be above the highest SLS concentration where CBZD is detected and below the lowest concentration where CBZD is no longer detected in the solid phase.

CSC Predicted from Cocrystal Aqueous Solubility and Micellar Solubilization of Cocrystal Components (Method 2)

Critical stabilization concentration was predicted from equations given in Table 1 (Eqs. 18, 24, and 26), with thermodynamic parameters measured in pure water or obtained from the literature. K_{sp} was calculated from cocrystal aqueous solubilities according to the equations given in Table 1 (Eqs. 13, 23, and 25 when $[M] = 0$); cocrystal aqueous solubilities were determined by measuring eutectic concentrations of the drug and the cofomer in pure water at $25 \pm 0.1^\circ\text{C}$. Cocrystals (50–100 mg) and CBZD (25–50 mg) were suspended in 3 mL of pure water up to 3 days. pH at equilibrium was measured, but not independently modified. Cocrystal aqueous solubility was calculated from eutectic concentration measurements according to $S_{RHA,aq} = \sqrt{[R]_{eu,aq} [A]_{eu,aq}}$ and

$S_{R_2H_2A,aq} = \sqrt[3]{\frac{[R]_{eu,aq} [A]_{eu,aq}}{4}}$ for 1:1 and 2:1 cocrystals, respectively. These equations consider ionization and micellar solubilization of cocrystal components. The evaluation of cocrystal solubilities and stabilities via eutectic points has been discussed thoroughly elsewhere.^{4,29,31} At the eutectic or transition point, the solution is saturated with respect to two solid phases, in this case, cocrystal and CBZD. This method allows for cocrystal solubility measurement under thermodynamic equilibrium that may not otherwise be accessible due to transformation to less soluble forms.

Micellar solubilization constants (K_s) for cocrystal components were determined by linear regression of the measured solubilities of the individual compo-

nents as a function of micellar SLS concentration at $25 \pm 0.1^\circ\text{C}$. K_a values were obtained from literature. Drug and cofomer concentrations were analyzed by high-performance liquid chromatography (HPLC). Solid phases at equilibrium were confirmed by XRPD.

CSC Measurement of Cocrystal Solubility in SLS Solutions (Method 3)

Critical stabilization concentration was evaluated by measuring cocrystal and drug solubilities as a function of SLS concentration in water at $25 \pm 0.1^\circ\text{C}$. Cocrystal solubilities were obtained by measuring eutectic concentrations of drug and cofomer in aqueous SLS solutions at $25 \pm 0.1^\circ\text{C}$. Cocrystal (50–100 mg) and CBZD (25–50 mg) were suspended in 3 mL of pure water up to 3 days. pH at equilibrium was measured, but not independently modified. Cocrystal solubilities were determined from the equations $S_{RHA,T} = \sqrt{[R]_{eu,T} [A]_{eu,T}}$ and $S_{R_2H_2A,T} = \sqrt[3]{\frac{[R]_{eu,T} [A]_{eu,T}}{4}}$ for 1:1 and 2:1 cocrystals, respectively. The equations consider ionization and micellar solubilization of cocrystal components. CBZD solubilities were measured as a function of SLS concentration in water at $25 \pm 0.1^\circ\text{C}$ and are consistent with the reported values.³² Drug and cofomer concentrations were analyzed by HPLC. Solid phases at equilibrium were confirmed by XRPD.

High-Performance Liquid Chromatography

The solution concentrations of CBZ and cofomer were analyzed by Waters HPLC (Milford, Massachusetts) equipped with an ultraviolet–visible spectrometer detector. Waters' operation software, Empower 2 (Waters), was used to collect and process the data. A C18 Thermo Electron Corporation (Quebec, Canada) column ($5 \mu\text{m}$, $250 \times 4.6 \text{ mm}$) at ambient temperature was used. The mobile phase composed of 55% methanol and 45% water with 0.1% trifluoroacetic acid, and the flow rate was 1 mL/min using an isocratic method. Injection sample volume was 20 or 40 μL . Absorbance of CBZ, SAC, SLC, SUC, and 4ABA was monitored at 284, 260, 303, 230, and 284 nm, respectively.

X-ray Powder Diffraction

X-ray powder diffraction diffractograms of solid phases were collected with a benchtop Rigaku Mini-flex X-ray diffractometer (Rigaku, Danvers, Massachusetts) using Cu $K\alpha$ radiation ($\lambda = 1.54 \text{ \AA}$), a tube voltage of 30 kV, and a tube current of 15 mA. Data were collected from 5° to 40° at a continuous scan rate of $2.5^\circ/\text{min}$.

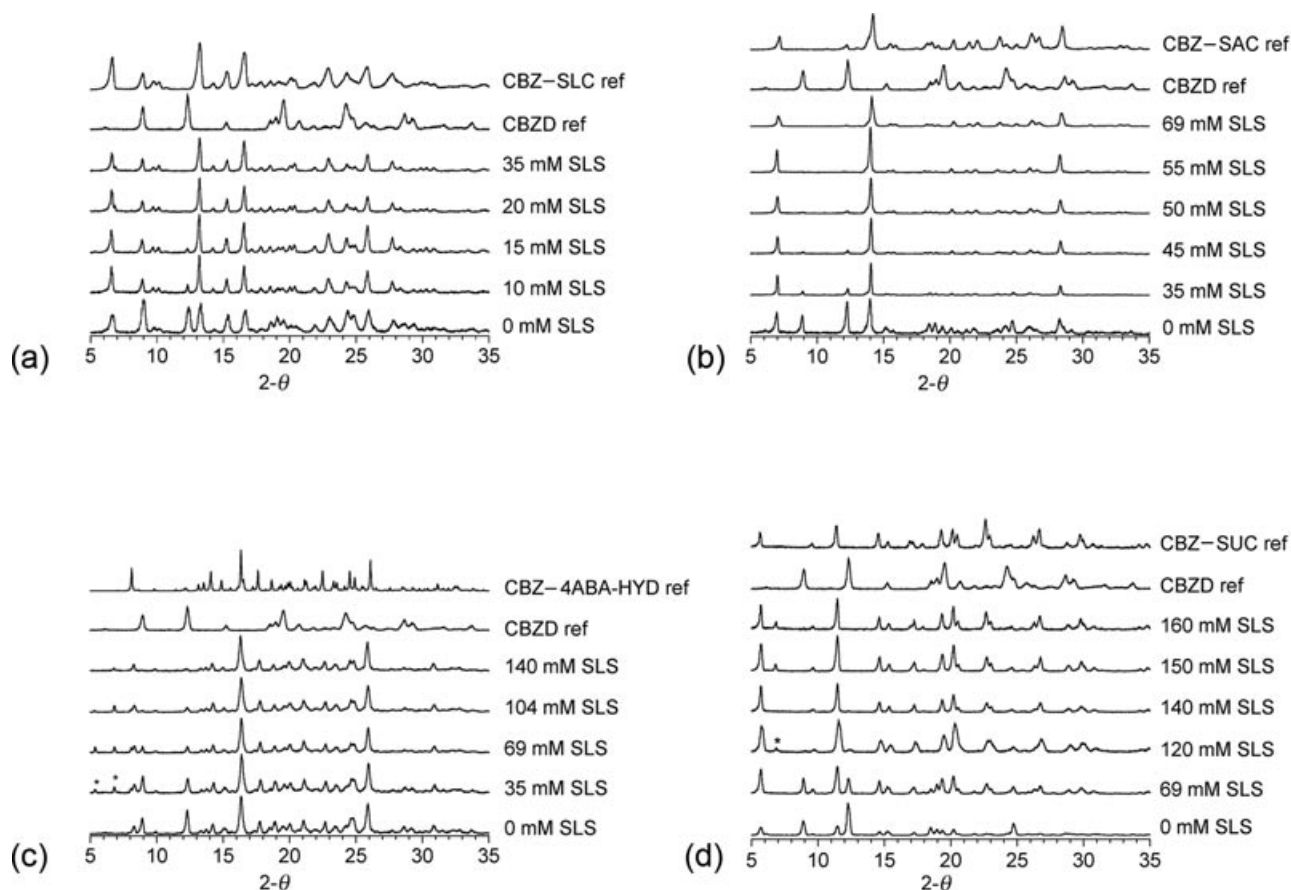


Figure 7. X-ray powder diffraction (XRPD) patterns showing the influence of SLS concentration on the cocrystal to drug conversion at 25°C for (a) CBZ-SLC at pH 3.0, (b) CBZ-SAC at pH 2.2, (c) CBZ-4ABA-HYD at pH 4.0, and (d) CBZ-SUC at pH 3.1. pH was not independently adjusted and represents the values measured at 24 h before solid phase recovery for XRPD analysis. Initial solid phase consisted of the cocrystal and a small fraction of CBZD. Peaks associated with SLS are indicated by *.

RESULTS

The equations presented in the theoretical section for cocrystal solubility in terms of micellar solubilization and ionization of cocrystal components suggest that cocrystal CSC and pH_{max} in micellar solutions can be *a priori* calculated from knowledge of cocrystal and drug solubilities in water, K_a and K_s values of cocrystal components, and surfactant CMC. At the CSC, cocrystals otherwise unstable in aqueous media will become thermodynamically stable. To evaluate the predictive power of the model, the solubility and stability of cocrystals of a nonionizable drug (CBZ) with cofomers of different ionization properties and stoichiometries were investigated as a function of SLS solution concentration. These included 1:1 cocrystals where cofomers are monoprotic weak acids (CBZ-SLC and CBZ-SAC) and 2:1 cocrystals with a diprotic weak acid (CBZ-SUC) or with an amphoteric cofomer (CBZ-4ABA-HYD). The cocrystal aqueous solubilities range from 1.32 mM for CBZ-SLC to 2.38 mM for CBZ-SUC (expressed in terms of drug concentration) at 25°C, or 2.5–4.5 times the solubility

of CBZD (0.53 mM).³² Cocrystal solubilities in pure water are in agreement with those reported in previous studies.²⁹

For cocrystals with ionizable components, the CSC is dependent on pH, and although the pH was not independently adjusted in these studies, the pH of surfactant solutions at equilibrium with solid phases was measured. The pH at the CSC corresponds to pH_{max} , where two solid phases (cocrystal and drug in this case) are in equilibrium with the solution.

The cocrystal CSCs were evaluated by three methods: (1) measurement of solid phase stability and pH as a function of SLS solution concentration, (2) calculation from cocrystal and drug solubility measurement in pure water, in conjunction with values of cocrystal component ionization (K_a), micellar solubilization (K_s), surfactant CMC, and solution pH, and (3) measurement of cocrystal solubility, drug solubility, and pH as a function of SLS solution concentration. Further, the dependence of CSC on pH_{max} was estimated from the evaluation of CSC at a single pH.

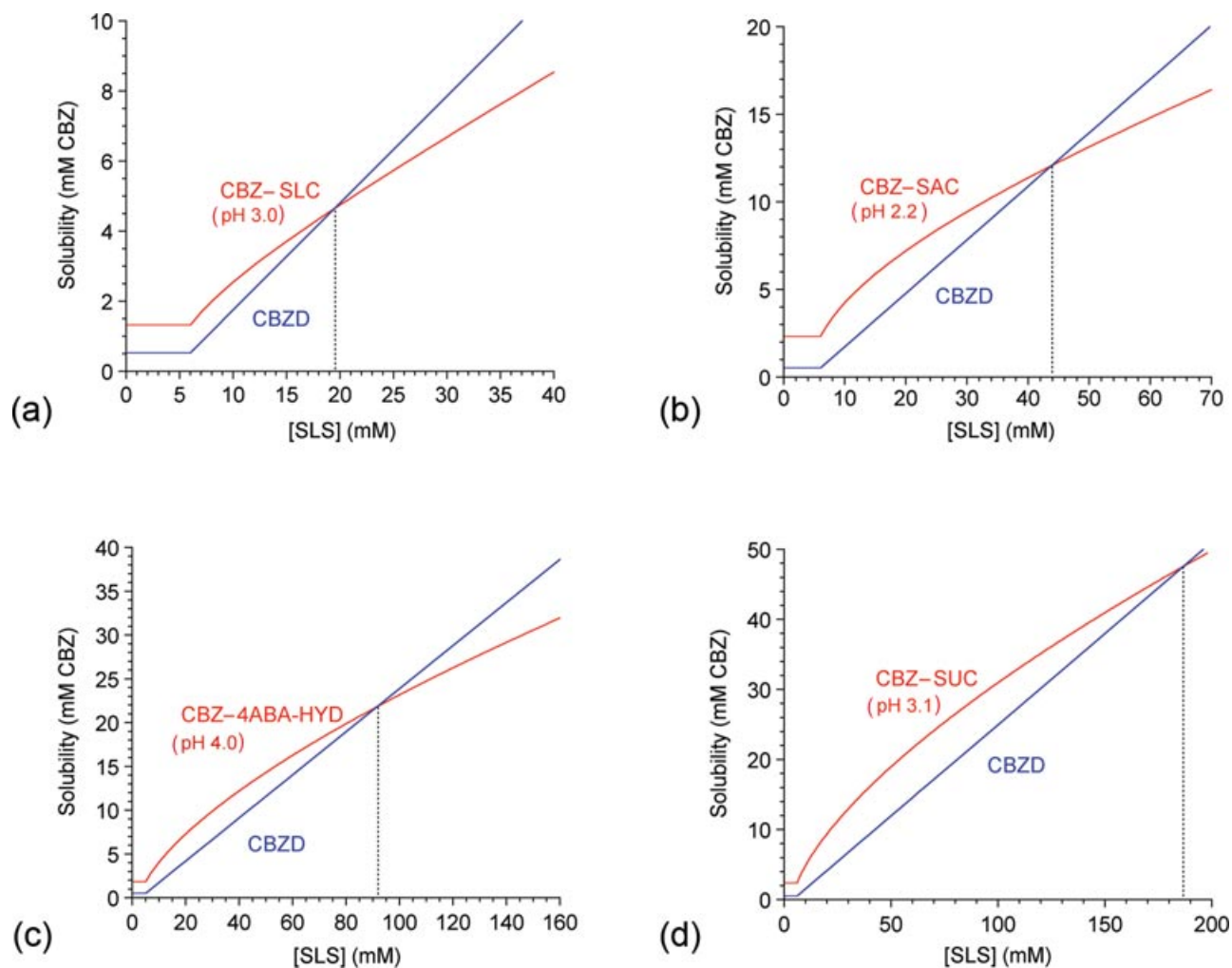


Figure 8. Calculated solubility and CSC of CBZ cocrystals in SLS aqueous solutions, from measured solubility in water and values of K_s , K_a , and pH listed in Table 2. Values of solution pH measured at equilibrium with solid phases are indicated. Dashed line shows the SLS concentration at the CSC, where the cocrystal and drug are thermodynamically stable. Solid lines represent solubility predictions for cocrystal and drug, according to Equations 13, 14, 23, and 25. A CMC value of 6 mM for SLS measured at saturation with CBZD was used in these calculations.

CSC from Measurement of Solid Phase Stability (Method 1)

Evaluation of the CSC from cocrystal phase stability measurements was carried out by XRPD analysis of solid phases after suspension in aqueous solutions of varying SLS concentration for 72 h, though 24 h was sufficient for equilibration to occur. Figure 7 shows that cocrystal conversion to drug (CBZD) decreases and becomes undetectable as surfactant concentration increases. An incremental variation of SLS concentrations for each cocrystal studied led to the following range of CSC values: CBZ-SLC 15 mM < CSC ≤ 20 mM, CBZ-SAC 50 mM < CSC ≤ 55 mM, CBZ-4ABA-HYD 69 mM < CSC ≤ 104 mM, and CBZ-SUC 120 mM < CSC ≤ 140 mM. The solution pH value associated with each CSC measurement is

reported in the legend of Figure 7. The CSC range for CBZ-SLC is in agreement with the previous results where the cocrystal was found to be stable in 35 mM (1%, w/v) SLS.¹⁹

Although the solid phase analysis approach is convenient for a quick assessment of the CSC range, it must be recognized that its accuracy is limited by the changes of solution composition from initial to equilibrium states as solid phase(s) dissolve and crystallize. It is also not sufficient to establish whether the stabilization achieved is of a thermodynamic or kinetic nature. These issues may be resolved by measuring the changes in solution composition that result from equilibration of the cocrystal and solid drug with the solution phase and/or calculating the CSC according to the equations presented here.

Table 2. Cocrystal K_{sp} and Drug Solubilities in Water, pK_a and K_s Values for Cocrystal Components in SLS Solutions Used in Calculation of CSC and pH_{max}

Solid Phase	K_{sp} (mM ² or mM ³)	pK_a	K_s^{CBZ} (mM ⁻¹)	$K_s^{coformer}$ (mM ⁻¹)	Aqueous Solubility (mM CBZ)
CBZ–SLC (1:1)	0.88	3.0 ^a	0.58 ^b	0.060	1.32 ± 0.06 (pH 3.0)
CBZ–SAC (1:1)	2.08	2.0 ^c	0.58 ^b	0.013	2.36 ± 0.05 (pH 2.2)
CBZ–4ABA–HYD (2:1)	2.56	2.6, 4.8 ^d	0.49 ^e	<0.010 ^f	1.83 ± 0.02 (pH 4.0)
CBZ–SUC (2:1)	6.15	4.1, 5.6 ^g	0.49 ^e	<0.010 ^f	2.38 ± 0.02 (pH 3.1)
CBZD	NA	N/A	0.49 (0–140 mM) 0.58 (0–50 mM)	n/a	0.53 ± 0.01 ^h

^aFrom Ref. 21.^bAverage K_s in lower concentrations of SLS (0–50 mM).^cFrom Refs. 22,23.^dFrom Ref. 25.^eAverage K_s in higher concentrations of SLS (0–140 mM).^f K_s values < 0.010 mM⁻¹ are considered equal to zero in calculations.^gFrom Ref. 24.^hFrom Ref. 32.

CSC from Measured Cocrystal Solubility in Pure Water (Method 2)

Figure 8 shows the calculated cocrystal and drug solubilities in micellar SLS solutions according to Equations 13, 23, and 25 for the cocrystal and Equation 14 for the drug, from thermodynamic parameter values presented in Table 2. The CSC where the cocrystal and CBZD are in equilibrium with the solution is given by the SLS concentration and pH at the intersection of the solubility curves. The pH at the CSC corresponds to the pH_{max} . CSC is strongly influenced by pH, and the calculations were carried out for pH values measured at saturation. This pH value changed by 0.2 units or less at the concentrations of SLS studied.

Predicted CSC values for these cocrystals range from 20 to 187 mM, which are in reasonably good agreement with the experimentally measured values listed in Table 3. Results of CSC measurement according to method 3 from solubility measurement in surfactant solutions are described in the next section.

The range of measured CSCs for each cocrystal by direct experimental measurement (methods 1 and 3) can be narrowed by examining smaller increments of SLS concentrations and by approaching equilibrium

from above and below saturation with respect to the cocrystal and drug phases. Estimation of CSC from thermodynamic properties of cocrystal and surfactant solutions (such as solubility in water, K_s , K_a , and CMC) provides useful guidance for the selection of surfactant, its concentration and solution pH, and decreases the number of experiments required by other methods.

Table 2 presents the thermodynamic parameter values for the CBZ cocrystals studied. Cocrystal K_{sp} in water and the corresponding solubility and pH are within 30% of those reported in previous studies.^{19,20,29} Coformer K_a values were obtained from the literature. Surfactant CMC and K_s values for the drug and coformer were determined from solubility measurements of individual components (drug or coformer) in SLS solutions. The CMC of SLS was experimentally measured to be 6 mM in solutions saturated with CBZ and is used in these calculations unless otherwise specified. The reported CMC value for SLS in water (8.3 mM, Ref.³³) is higher than the value measured in this study and those reported for CBZ solutions without coformer (5.3 mM, Ref.³²). The purity, ionic strength, and interactions with the solutes are well documented to induce changes in the CMC of ionic surfactants.^{9,34–36} K_s values for hydrophobic

Table 3. Critical Stabilization Concentrations and Solubilities of CBZ Cocrystals in SLS Aqueous Solutions

Cocrystal	pH	$S_{cocrystal}/S_{drug}$ in Terms of CBZ (mM)	CSC (SLS mM)		
			Measured from Solid Phase Stability in SLS Solutions (Method 1) ^a	Predicted from Measured Cocrystal Solubility in Water (Method 2) ^b	Measured from Cocrystal Solubility in SLS Solutions (Method 3) ^c
CBZ–SLC (1:1)	3.0	2.5	15 < CSC ≤ 20	23 (CMC = 9 mM) 20 (CMC = 6 mM)	18 < CSC < 27
CBZ–SAC (1:1)	2.2	4.5	50 < CSC ≤ 55	44	35 < CSC < 50
CBZ–4ABA–HYD (2:1)	4.0	3.5	69 < CSC ≤ 104	92	70 < CSC < 140
CBZ–SUC (2:1)	3.1	4.5	120 < CSC ≤ 140	187	140 < CSC

^aMethod 1: CSCs determined from XRPD analysis of the solid phase in Figure 7. The lower boundary is the highest concentration of SLS where CBZD is detected in the solid phase, and the upper boundary is the lowest concentration of SLS where no CBZD is detected in the solid phase.^bMethod 2: CSCs calculated according to Equations 18, 24, and 26 given in Table 1, from K_{sp} , pK_a , and K_s values in Table 2.^cMethod 3: CSCs determined from measurement of cocrystal and drug solubilities in SLS solutions (Figure 9–11).

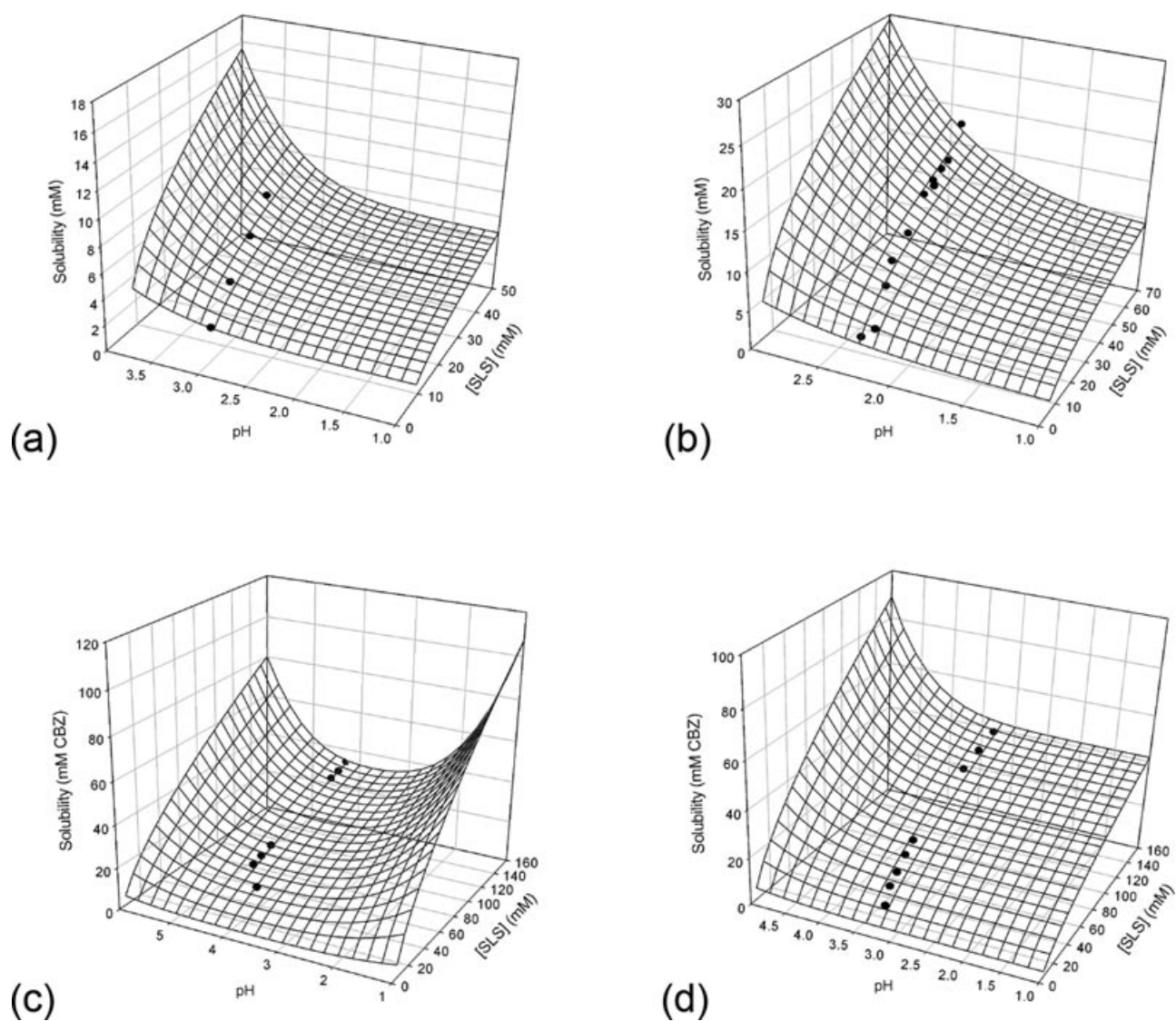


Figure 9. Influence of pH and surfactant concentration on cocystal solubility for (a) CBZ-SLC, (b) CBZ-SAC, (c) CBZ-4ABA-HYD, and (d) CBZ-SUC. Circles represent cocystal solubilities measured in surfactant solutions, whereas surfaces represent cocystal solubilities calculated from Equations 13, 23, and 25 using measured cocystal solubility in water at a given pH and thermodynamic values listed in Table 2.

compounds have been reported to be influenced by the solute and surfactant concentrations.^{9,37–41} K_s values as well as the concentration ranges in which they were measured is shown in Table 2. An expression that describes the K_s dependence on surfactant concentration could also be used for more accurate predictions.

CSC from Measured Cocystal Solubility in SLS Solutions

Figure 9 shows the experimental and predicted cocystal solubility dependence on surfactant concentration and pH. The pH was not independently adjusted, and experimental measurements represent the narrow pH range of micellar solutions saturated with the cocystal. Changes in pH, however, can profoundly affect the cocystal solubility as indicated by

the surfaces predicted from Equations 13, 14, 23, and 25 using parameter values given in Table 2. Cofomer ionization, in this case, determines the shape of the curves because the drug is not ionizable and the cofomer is not solubilized by micelles. The solubility of cocystals with acidic cofomers increases with the pH, whereas solubility decreases and increases with an amphoteric cofomer. The contribution of cofomer ionization to cocystal solubility is consistent with the behavior in water, which we previously reported.⁴

Figures 10 and 11 show the predicted and measured cocystal and drug solubilities as a function of surfactant concentration. The CMC for SLS was constant at 6 mM for cocystals in Figure 9, whereas a CMC of 9 mM was estimated from the solubility of

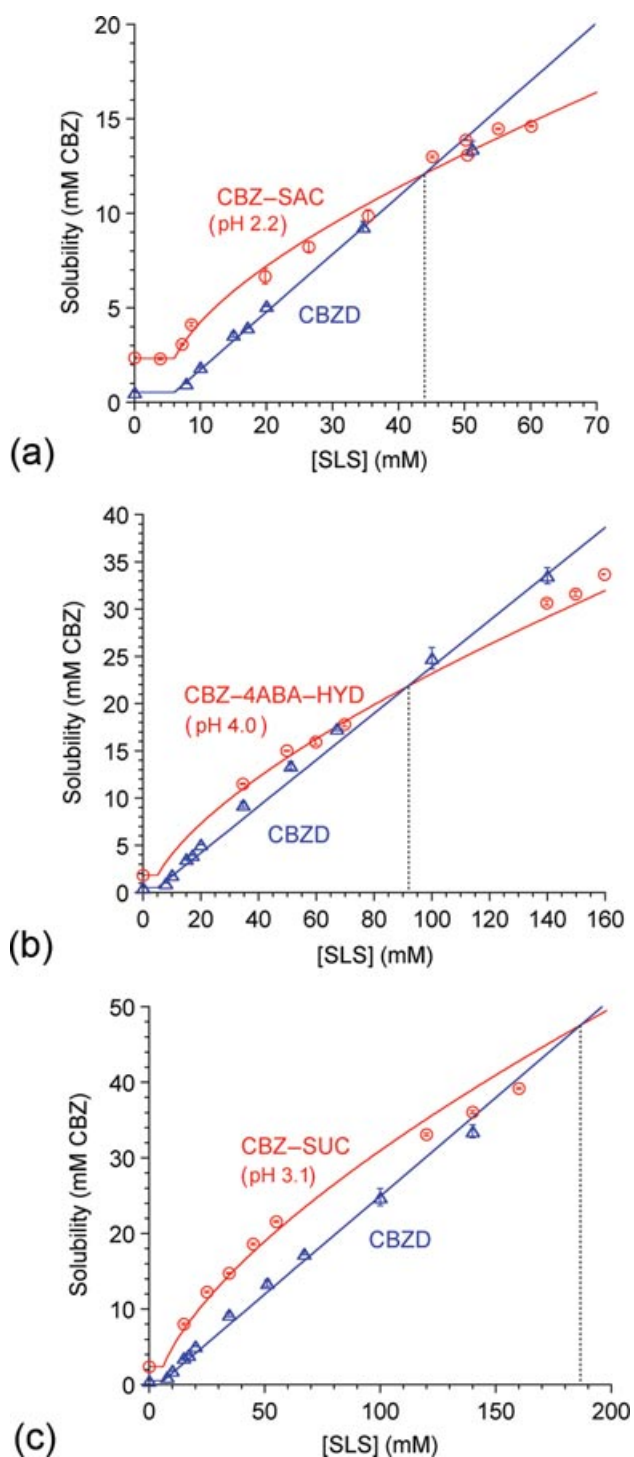


Figure 10. Experimental and predicted influence of SLS on drug (CBZD) solubility and CBZ cocrystal solubilities for (a) CBZ-SAC, (b) CBZ-4ABA-HYD, and (c) CBZ-SUC. Experimental solubilities were measured in unbuffered surfactant aqueous solutions. The pH measured at equilibrium is indicated. Symbols (circles and triangles) represent the experimental values. Predicted drug and cocrystal solubilities (solid lines) were calculated according to Equations 13, 14, 23, and 25, with thermodynamic values listed in Table 2. The CSC is indicated by the SLS concentration (dashed line) at the intersection of the predicted cocrystal and drug solubility curves.

CBZ-SLC cocrystal (Fig. 10). Results show very good agreement between the predicted and experimental cocrystal solubility and CSC behavior. The largest deviations were observed with the CBZ-SUC cocrystal at high SLS concentration and may be a result of changes in K_s with surfactant and cofomer concentrations. The CSC values obtained by the three methods are listed in Table 3 and show very good agreement between the predicted (method 2) and experimentally measured CSC values (methods 1 and 3). A small variation in the CMC of SLS, such as from 6 mM to 9 mM for CBZ-SLC, has a relatively minor impact on the CSC (20–23 mM).

Improving the predictive power of the model requires more rigorous consideration of various solution interactions on equilibrium constants (such as K_a and K_s) and on the surfactant properties (such as CMC). The model equations assume that solubilization of one cocrystal component is unaffected by the presence of the other; that is, K_s for a component under pure conditions is a good approximation for the K_s in the presence of a cocrystal. Factors that cause K_s , K_a , and CMC to change (such as ionic strength) influence the predictions, and these differences may be considered by measuring the parameters as a function of solution composition. A 0.2-unit pH or pK_a change when $pH \approx pK_a$ (e.g., CBZ-SAC) can lead to errors in the CSC of the order of 15%–30%, and even greater errors when $pH > pK_a$. A 10% error in K_s^{CBZ} (e.g., CBZ-SUC) leads to an error of 10% in the CSC.

An alternative approach would have been to fit the models to the experimental data and evaluate the corresponding parameters. Given that this is the first manuscript on this topic, we chose to use the thermodynamic parameter values reported in the literature or measured for single components of cocrystals to evaluate the predicted cocrystal solubilities and CSC values with all the established assumptions.

CSC and pH_{max} Dependence on Cocrystal and Surfactant Properties

The treatment developed in the theoretical section is based on cocrystal component ionization and micellar solubilization. This treatment identified the existence of a CSC and the factors that determine its value: (1) cocrystal K_{sp} and solubility relative to drug, (2) ionization of cocrystal components, (3) micellar solubilization of cocrystal components, (4) cocrystal stoichiometry, and (5) surfactant CMC. CSC is predicted to increase with increasing cocrystal solubility, ionization, cofomer K_s , and surfactant CMC and with decreasing drug K_s .

For this series of CBZ cocrystals, the magnitude of the CSC is mostly influenced by the cocrystal K_{sp} , stoichiometry, and cofomer ionization. Between cocrystals of the same stoichiometry such as CBZ-SLC and

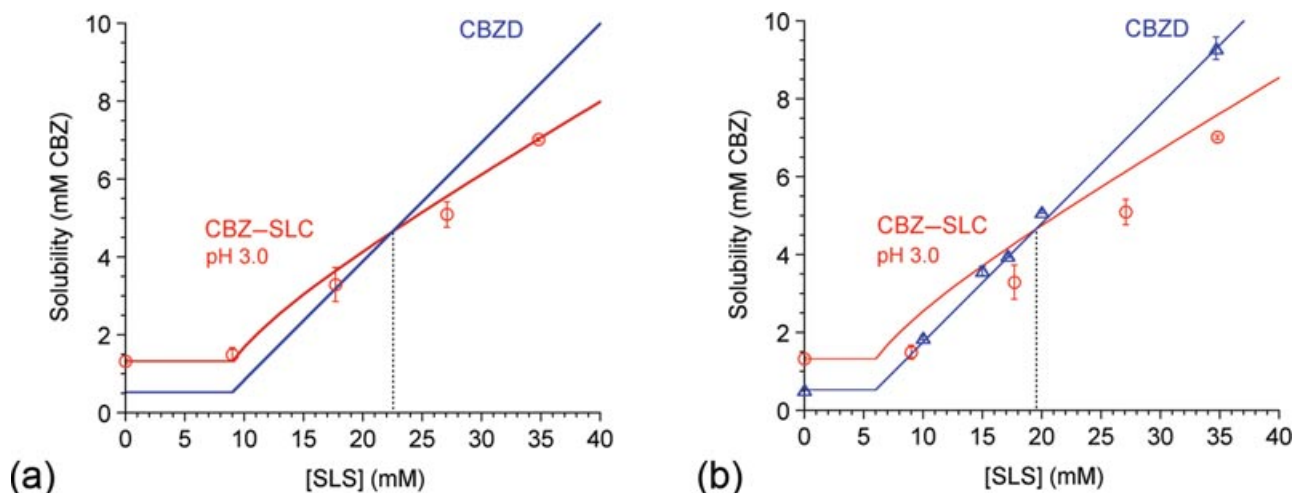


Figure 11. Influence of SLS on the solubility of CBZ-SLC and CBZD. The lines represent predictions according to Equations 13 and 14 from two different CMC values: (a) 9 mM and (b) 6 mM. Symbols (circles and triangles) represent the experimental values.

CBZ-SAC, the experiments confirm the prediction that higher solubility relative to the drug results in a higher CSC (Table 3). These have similar percentage ionized (since $\text{pH} \approx \text{pK}_a$ of the cofomer), and $K_s^{\text{HA}} \ll K_s^{\text{R}}$. The CSC is mainly determined by the cocystal solubility relative to the drug. Similar behavior is observed for 2:1 cocystals CBZ-4ABA-HYD and CBZ-SUC. These cocystals have low levels of ionization under the pH conditions studied (10%–20% of the cofomer ionized), and negligible cofomer solubilization. The experiments also show that the 2:1 cocystal CBZ-SUC has a higher CSC than the 1:1 cocystal

CBZ-SAC of equal solubility (in terms of CBZ moles). The higher CSC of drug rich stoichiometries is a consequence of the higher surfactant concentrations required to solubilize more drugs to achieve the same level of cofomer enrichment in the aqueous pseudo phase as a 1:1 cocystal.

The pH value at the CSC is pH_{max} , where the cocystal and drug, in this case, are in equilibrium with solution. The predicted CSC and pH_{max} values for the CBZ cocystals studied are plotted in Figure 12. These were calculated from Equations 18, 24, and 26 using values presented in Table 2. CSC is shown to be strongly dependent on pH and follows the cofomer ionization behavior. It is recognized that these calculations assume that ionized components do not interact with the micelles and that K_a , K_s , and CMC are independent of solution composition.

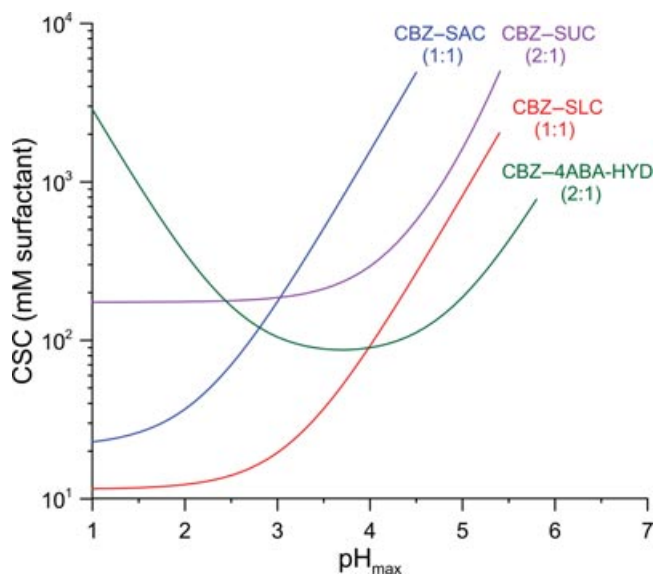


Figure 12. Calculated CSC (mM SLS) and pH_{max} for CBZ cocystals according to Equations 18, 24, and 26 using measured values presented in Table 2. CSC dependence on pH may be tailored based on the ionization properties of the cofomer.

CONCLUSIONS

A theoretical treatment that considers the contributions of cocystal dissociation, component ionization, and micellar solubilization demonstrates that surfactants can impart thermodynamic stability to cocystals that otherwise convert to parent drug solid in aqueous solutions. The CSC and pH_{max} represent the surfactant concentration and solution pH where the cocystal is in thermodynamic equilibrium with the solid drug and solution phases. Therefore, both CSC and pH_{max} (in the case of ionizable cocystal components) are key indicators of cocystal stability. This behavior is confirmed by the stabilization of several CBZ cocystals in SLS micellar solutions.

How effective a surfactant is in changing the thermodynamic stability of a cocystal, CSC, and pH_{max} is determined mostly by the differential solubilization

of cocrystal components by micelles. Such differential solubilization of cocrystal components leads to a lower rate of solubility increase with surfactant micellar concentration for the cocrystal, compared with that of the drug solubility increase (when the drug has superior micellar solubilization of cocrystal components).

For cocrystals of nonionizable, hydrophobic drugs with ionizable, hydrophilic cofomers, the theoretical treatment predicts that surfactant CSC is decreased by: (1) preferential drug solubilization ($K_s^R \gg K_s^{HA}$), (2) low ionization of cofomer, (3) low cocrystal aqueous solubility relative to drug, and (4) cocrystal stoichiometries that are lower in drug than cofomer. This generalization assumes that there is no additional solution complexation and that ionized cofomer is not solubilized by the micelles. The relationship between CSC and pH_{max} is determined by the ionization behavior of the cofomer, with CSC changing orders of magnitude at pH values where cofomer ionizes. Acidic cofomers exhibit an increase in pH_{max} with increasing surfactant concentration, whereas amphoteric cofomers exhibit pH_{max} decrease and increase.

Critical stabilization concentration and pH_{max} for cocrystals in micellar solutions are quantitatively predicted by mathematical models from solution phase properties of cocrystal (K_{sp}), cocrystal components (K_s and K_a), and surfactant (CMC). CSC, pH_{max} , and cocrystal solubility predicted by the models are in very good agreement with the experimental measurements. The proposed models provide a rational basis for selecting additives and solution conditions to achieve desired cocrystal solubility/stability from parameter values that are generally available in the literature or experimentally accessible. Because cocrystals owe their solubility to the ionization and association of their components in solution, it is essential to consider the influence of solution conditions such as pH and presence of surfactants and other additives for meaningful cocrystal assessment and selection.

ACKNOWLEDGMENTS

We gratefully acknowledge the financial support from the Warner-Lambert/Parke Davis Fellowship and the Upjohn Fellowship from the College of Pharmacy, the University of Michigan.

REFERENCES

1. Fleischman SG, Kuduva SS, McMahon JA, Moulton B, Walsh RDB, Rodríguez-Hornedo N, Zaworotko MJ. 2003. Crystal engineering of the composition of pharmaceutical phases: Multiple-component crystalline solids involving carbamazepine. *Cryst Growth Des* 3(6):909–919.
2. Childs SL, Hardcastle KI. 2007. Cocrystals of piroxicam with carboxylic acids. *Cryst Growth Des* 7(7):1291–1304.
3. Nehm SJ, Rodríguez-Spong B, Rodríguez-Hornedo N. 2006. Phase solubility diagrams of cocrystals are explained by solubility product and solution complexation. *Cryst Growth Des* 6(2):592–600.
4. Bethune SJ, Huang N, Jayasankar A, Rodríguez-Hornedo N. 2009. Understanding and predicting the effect of cocrystal components and pH on cocrystal solubility. *Cryst Growth Des* 9(9):3976–3988.
5. Jayasankar A, Reddy LS, Bethune SJ, Rodríguez-Hornedo N. 2009. Role of cocrystal and solution chemistry on the formation and stability of cocrystals with different stoichiometry. *Cryst Growth Des* 9(2):889–897.
6. Remenar JF, Peterson ML, Stephens PW, Zhang Z, Zimenkov Y, Hickey MB. 2007. Celecoxib:Nicotinamide dissociation: Using excipients to capture the cocrystal's potential. *Mol Pharm* 4(3):386–400.
7. McNamara DP, Childs SL, Giordano J, Iarriccio A, Cassidy J, Shet MS, Mannion R, O'Donnell E, Park A. 2006. Use of a glutaric acid cocrystal to improve oral bioavailability of a low solubility API. *Pharm Res* 23(8):1888–1897.
8. Yadav AV, Dabke AP, Shete AS. Crystal engineering to improve physicochemical properties of mefloquine hydrochloride. *Drug Dev Ind Pharm* 36(9):1036–1045.
9. Christian SD, Scamehorn JF. 1995. Solubilization in surfactant aggregates. Marcel Dekker, Inc., New York, New York.
10. Strickley RG. 2004. Solubilizing excipients in oral and injectable formulations. *Pharm Res* 21(2):201–230.
11. Wiedmann TS, Kamel L. 2002. Examination of the solubilization of drugs by bile salt micelles. *J Pharm Sci* 91(8):1743–1764.
12. Wiedmann TS, Bhatia R, Wattenberg LW. 2000. Drug solubilization in lung surfactant. *J Control Release* 65(1–2):43–47.
13. Serajuddin ATM, Sheen P-C, Mufson D, Bernstein DF, Augustine MA. 1988. Physicochemical basis of increased bioavailability of a poorly water-soluble drug following oral administration as organic solutions. *J Pharm Sci* 77(4):325–329.
14. Serajuddin ATM. 1999. Solid dispersion of poorly water-soluble drugs: Early promises, subsequent problems, and recent breakthroughs. *J Pharm Sci* 88(10):1058–1066.
15. Rodríguez-Hornedo N, Nehm SJ, Jayasankar A. 2006. Cocrystals: Design, properties and formation mechanisms. In *Encyclopedia of Pharmaceutical Technology*, Eds. Swarbrick and Boylan, Informa Health Care, London; 3rd ed. pp 615–635.
16. Rodríguez-Hornedo N, Nehm SJ, Seefeldt KF, Pagan-Torres Y, Falkiewicz CJ. 2006. Reaction crystallization of pharmaceutical molecular complexes. *Mol Pharm* 3:362–367.
17. Bak A, Gore A, Yanez E, Stanton M, Tufekcic S, Syed R, Akrami A, Rose M, Surapaneni S, Bostick T, King A, Neervannan S, Ostovic D, Koparkar A. 2008. The co-crystal approach to improve the exposure of a water-insoluble compound: AMG 517 sorbic acid co-crystal characterization and pharmacokinetics. *J Pharm Sci* 97(9):3942–3956.
18. Schultheiss N, Newman A. 2009. Pharmaceutical cocrystals and their physicochemical properties. *Cryst Growth Des* 9(6):2950–2967.
19. Huang N, Rodríguez-Hornedo N. 2010. Effect of micellar solubilization on cocrystal solubility and stability. *Cryst Growth Des* 10(5):2050–2053.
20. Huang N, Rodríguez-Hornedo N. 2011. Engineering cocrystal thermodynamic stability and eutectic points by micellar solubilization and ionization. *CrystEngComm* 13(17):409–5422.
21. Nordström FL, Rasmuson ÅC. 2006. Solubility and melting properties of salicylic acid. *J Chem Eng Data* 51(5):1668–1671.
22. Williamson DS, Nagel DL, Markin RS, Cohen SM. 1987. Effect of pH and ions on the electronic structure of saccharin. *Food Chem Toxicol* 25(3):211–218.
23. Kojima S, Ichigabase H, Iguchi S. 1966. Studies on sweetening agents. VII. Absorption and excretion of sodium cyclamate (2). *Chem Pharm Bull* 14(9):965–971.

24. O'Neil M, Smith A, Heckelman P, Budavari S. 2001. The Merck Index. 13th ed. New York: John Wiley and Sons.
25. Robinson RA, Biggs AI. 1957. The ionization constants of p-aminobenzoic acid in aqueous solution at 25°C. *Aust J Chem* 10(2):128–134.
26. Li P, Tabibi SE, Yalkowsky SH. 1998. Combined effect of complexation and pH on solubilization. *J Pharm Sci* 87(12):1535–1537.
27. Jain A, Ran YQ, Yalkowsky SH. 2004. Effect of pH-sodium lauryl sulfate combination on solubilization of PG-300995 (an anti-HIV agent): A technical note. *AAPS PharmSciTech* 5(3):65–67.
28. He Y, Yalkowsky SH. 2006. Solubilization of monovalent weak electrolytes by micellization or complexation. *Int J Pharm* 314(1):15–20.
29. Good DJ, Rodríguez-Hornedo N. 2009. Solubility advantage of pharmaceutical cocrystals. *Cryst Growth Des* 9(5):2252–2264.
30. Bethune SJ. 2009. Thermodynamic and kinetic parameters that explain crystallization and solubility of pharmaceutical cocrystals. PhD Thesis; University of Michigan, Ann Arbor, MI.
31. Good DJ, Rodríguez-Hornedo N. 2010. Cocrystal eutectic constants and prediction of solubility behavior. *Cryst Growth Des* 10(3):1028–1032.
32. Rodríguez-Hornedo N, Murphy D. 2004. Surfactant-facilitated crystallization of dihydrate carbamazepine during dissolution of anhydrous polymorph. *J Pharm Sci* 93(2):449–460.
33. Mukerjee P, Mysels KJ. 1971. Critical micelle concentrations of aqueous surfactant systems. Washington, District of Columbia: US National Bureau of Standards.
34. Crison JR, Weiner ND, Amidon GL. 1997. Dissolution media for *in vitro* testing of water-insoluble drugs: Effect of surfactant purity and electrolyte on *in vitro* dissolution of carbamazepine in aqueous solutions of sodium lauryl sulfate. *J Pharm Sci* 86(3):384–388.
35. Seedher N, Kanojia M. 2008. Micellar solubilization of some poorly soluble antidiabetic drugs: A technical note. *AAPS PharmSciTech* 9(2):431–436.
36. Aburub A, Risley DS, Mishra D. 2008. A critical evaluation of fasted state simulating gastric fluid (FaSSGF) that contains sodium lauryl sulfate and proposal of a modified recipe. *Int J Pharm* 347(1–2):16–22.
37. Moroi Y. 1992. *Micelles: Theoretical and applied aspects*. Plenum Press, New York, New York.
38. Rangel-Yagui CO, Junior AP, Tavares LC. 2005. Micellar solubilization of drugs. *J Pharm Sci* 8(2):147–163.
39. Pennell KD, Adinolfi AM, Abriola LM, Diallo MS. 1997. Solubilization of dodecane, tetrachloroethylene, and 1,2-dichlorobenzene in micellar solutions of ethoxylated nonionic surfactants. *Environ Sci Technol* 31(5):1382–1389.
40. Stilbs P. 1983. A comparative study of micellar solubilization for combinations of surfactants and solubilizates using the Fourier transform pulsed-gradient spin-echo NMR multicomponent self-diffusion technique. *J Colloid Interface Sci* 94(2):463–469.
41. Hayworth JS, Burris DR. 1997. Nonionic surfactant-enhanced solubilization and recovery of organic contaminants from within cationic surfactant-enhanced sorbent zones. 1. Experiments. *Environ Sci Technol* 31(5):1277–1283.